

Dynamically reversible and strong circular dichroism based on Babinet-invertible chiral metasurfaces

Xiaoqing Luo^{1,2}, Fangrong Hu³, and Guangyuan Li^{1,2,4,*}

¹CAS Key Laboratory of Human-Machine Intelligence-Synergy Systems, Shenzhen Institutes of Advanced Technology, Chinese Academy of Sciences, Shenzhen, 518055 China

²Guangdong-Hong Kong-Macao Joint Laboratory of Human-Machine Intelligence-Synergy Systems, Chinese Academy of Sciences, Shenzhen Institutes of Advanced Technology, Shenzhen 518055, China

³Guangxi Key Laboratory of Optoelectronic Information Processing, Guilin University of Electronic Technology, Guilin 541004, China

⁴Shenzhen College of Advanced Technology, University of Chinese Academy of Sciences, Shenzhen 518055, China

*Corresponding author: gy.li@siat.ac.cn

Abstract

We propose a Babinet-invertible chiral metasurface for achieving dynamically reversible and strong circular dichroism (CD). The proposed metasurface is composed of VO₂-metal hybrid structure, and when VO₂ transits between the dielectric state and the metallic state, the metasurface unit cell switches between complementary structures that are designed according to the Babinet principle. This leads to a large and reversible CD tuning range between ± 0.5 at 0.97 THz, which is larger than the literature. We attribute the CD effect to extrinsic chirality of the proposed metasurface. We envision that the Babinet-invertible chiral metasurface proposed here will advance the engineering of active and tunable chiro-optical devices and promote their applications.

Manipulation of optical chirality has a diverse range of applications, such as polarization conversion [1], bio-sensing [2], polarization-sensitive spectrometry [3, 4], and telecommunications [5]. Chiral metamaterial emerges as a new and exciting platform for providing remarkable chiro-optical effects including circular dichroism [6], optical activity [7] and asymmetric transmission [8]. Among these, circular dichroism (CD) manifests itself as a difference between the transmittances for the left- and right-handed circularly polarized (LCP and RCP) waves, which can be calculated with

$$CD = T_{\text{LCP}} - T_{\text{RCP}}, \quad (1)$$

where T_{LCP} and T_{RCP} are the transmittances of the LCP and the RCP waves, respectively. Making use of circular dichroism, broadband circular polarizers [9] and chiral beam splitters [10] have been demonstrated.

Over the years, interest has shifted from how to increase the chiral optical response into how to realize switchable chirality under a certain external stimulus [11]. In order to achieve dynamic tuning of CD, one approach is to reconfigure the structural geometry [12]. This is usually achieved by using reconfigurable 3D plasmonic metamolecules. For example, Kuzyk *et al.* [13] proposed reconfigurable three-dimensional plasmonic metamolecules and demonstrated reversible CD through DNA-regulated conformational changes at the nanoscale. Lan *et al.* [14] also demonstrated dynamical tuning of CD through DNA-guided structural reconfiguration of self-assembled gold nanorod helix superstructures. To remove the need for geometrical reconfiguration, in 2012 Zhang *et al.* [15] demonstrated optically controlled CD switching between -0.3 and 0.3 in a 3D chiral terahertz metamaterial with embedded photo-active silicon. Since then metamaterials incorporating active materials, such as silicon, graphene and phase change materials, have been the focus for dynamical tuning of CD effect. For example, Kenannakis *et al.* [16] proposed a bi-layer uniaxial chiral metamaterial incorporating photoconducting Si and showed that CD between 0 and 0.16 can be dynamically tuned under external optical pumping. Yin *et al.* [17] demonstrated reversal of the circular dichroism sign (between -0.1 and 0.2) in layered plasmonic chiral metamaterial incorporating phase change material $\text{Ge}_3\text{Sb}_2\text{Te}_6$. Lv *et al.* [18] proposed two 90° twisted E-shaped resonators with embedded vanadium dioxide (VO_2) and achieved a complete switching effect of CD with a maximum change of 0.45 at around 1.36 THz. Wang *et al.* [19] also proposed bi-layer hybrid metamaterials integrated with vanadium dioxide (VO_2) showing switchable CD between 0 and 0.4 . However, these 3D chiral structures are bulky, and difficult to fabricate and integrate.

Since the first experimental demonstration by Papakostas *et al.* [20], planar metasurfaces, which are much easier to fabricate and integrate compared with the above 3D chiral metamaterials, and which exhibit extrinsic chirality under oblique incidence, have been a promising platform for achieving large CD [21–24]. By further incorporating active materials such as graphene, Huang *et al.* [25] proposed a graphene–metal hybrid chiral metasurface and achieved reversible CD between -0.05 and 0.04 in the mid-infrared regime by varying the Fermi energy of graphene. Zhou *et al.* [26] also proposed a graphene metasurface and showed reversible and large CD between -0.25 and 0.4 . However, these CD tuning ranges are relatively small, hindering the potential applications.

In this letter, we tackle this challenge by proposing a Babinet-invertible chiral metasurface for achieving dynamically switchable and large circular dichroism chiral metasurface based on Babinet’s principle. We will show that by changing the phase of VO_2 between the dielectric state and the metallic state, which can be done thermally, optically or electrically [27], the CD can be tuned between 0.5 and -0.5 at 0.97 THz. This CD tuning range is larger compared with the above 3D metamaterials [15–19] and planar metasurfaces [25, 26]. The operation principle will be clarified based on the Babinet’s principle and extrinsic chirality. The effects of the VO_2 conductivity on the CD tuning performance will also be investigated.

Figure 1 illustrates the proposed Babinet-invertible chiral metasurface composed of hybrid gold- VO_2 structures on top of a high-resistivity silicon substrate. When VO_2 is in the dielectric state, denoted as “ $\text{VO}_2(\text{D})$ ” and in green, the interactions between the VO_2 structures and the incident terahertz wave are negligible compared with those between the gold structures and the terahertz wave, thus the metasurface unit cell is effectively composed of the left-top and right-bottom U-shaped gold ridges, as illustrated in the red dashed box in Fig. 1(c). In this scenario, LCP terahertz wave can transmit through the metasurface whereas RCP wave is blocked, suggesting strong circular dichroism effect, as illustrated by Fig. 1(a).

When VO_2 is in the metallic state, denoted as “ $\text{VO}_2(\text{M})$ ” and in brown, VO_2 behaves like gold. If we approximately treat metallic VO_2 as gold and shift the unit cell in Fig. 1(c) by half a period, the equivalent metasurface unit cell is composed of the left-top and right-bottom U-shaped

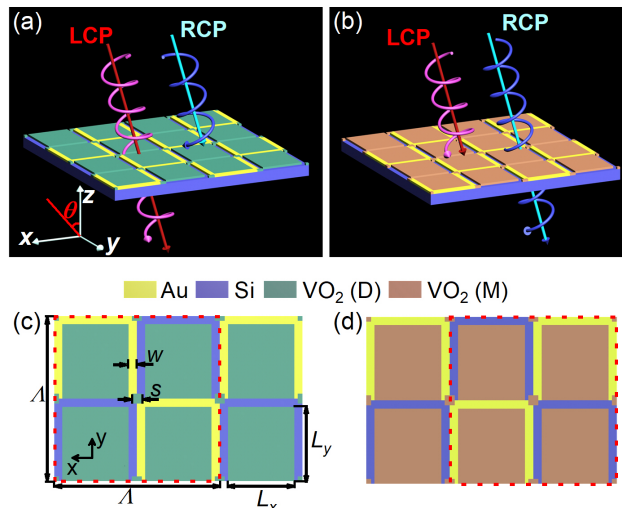


Figure 1: Schematics of the proposed Babinet-invertible chiral metasurface for achieving reversible and strong CD effect. (a) When VO_2 is in the dielectric state (in green, denoted as “ $\text{VO}_2(\text{D})$ ”), LCP terahertz wave transmits through the metasurface while RCP wave is blocked. (b) When VO_2 is in the metallic state (in brown, denoted as “ $\text{VO}_2(\text{M})$ ”), LCP wave transmits through the metasurface while RCP wave is blocked. (c)(d) Top views of the metasurface unit cells (in dashed boxes) for $\text{VO}_2(\text{D})$ and $\text{VO}_2(\text{M})$, respectively. $\Lambda = 100 \mu\text{m}$, $w = 7 \mu\text{m}$, $L_x = L_y = 36 \mu\text{m}$, $s = 8 \mu\text{m}$.

slots in a gold film, as illustrated in the red dashed box in Fig. 1(d). Comparing the effective unit cells in Figs. 1(c)(d), we find these are exactly complementary structures. According to the Babinet’s principle [28], RCP terahertz wave will transmit through the metasurface whereas LCP wave will be blocked in this scenario, as illustrated by Fig. 1(b). Therefore, taking advantage of the Babinet’s principle, the proposed Babinet-invertible chiral metasurface can exhibit reversible circular dichroism effect.

The reversible polarization dependent transmission performance was numerically evaluated using the frequency-domain solver in CST Microwave Studio. Frequency-dependent transmission is obtained as $t(f) = S_{12}(f)$, and the corresponding transmittance is then calculated with $T = |t|^2$. In the simulations, we take the periods of the metasurface unit cell in both x and y directions to be $\Lambda = 100 \mu\text{m}$, and take the thicknesses of gold and VO_2 be 200 nm and 400 nm , respectively. Unless otherwise specified, the incident angle is set to be $\theta = 60^\circ$. We adopted frequency-dependent permittivities of lossy gold and loss-free silica substrate from the build-in material library. Drude model was adopted to describe the frequency-dependent permittivities of VO_2 in the terahertz regime [29],

$$\varepsilon(\omega) = \varepsilon_\infty - \frac{\omega_p^2(\sigma)}{\omega^2 + i\gamma\omega} \quad (2)$$

where ε_∞ is the permittivity at high frequency limit, $\omega_p(\sigma)$ is the conductivity-dependent plasmon frequency, σ is the conductivity, and $\gamma = 5.75 \times 10^{13} \text{ rad/s}$ is the collision frequency assumed to be independent of the conductivity. A further examination reveals that $\omega_p^2(\sigma)$ can be approximately expressed as $\omega_p^2(\sigma) = (\sigma/\sigma_0) \cdot \omega_p^2(\sigma_0)$ with $\omega_p(\sigma_0) = 1.4 \times 10^{15} \text{ rad/s}$ for $\sigma_0 = 3 \times 10^5 \text{ S/m}$ [29]. For VO_2 in the dielectric and the metallic states, we take σ to be 40 S/m and $4 \times 10^5 \text{ S/m}$, respectively.

Figure 2(a) shows that when VO_2 is in the dielectric state, the transmission decreases as the operation frequency increases for both the LCP and the RCP terahertz waves. There exists a pronounced dip locating at frequency of $f = 0.94 \text{ THz}$ for the RCP wave. When VO_2 is in the metallic state, however, the transmission spectra behave reversely: the transmission increases with the frequency, and there is a transmission peak at $f = 0.96 \text{ THz}$ for the RCP wave, as shown in Fig. 2(b). The peak transmission frequency is slightly blue shifted by 2% compared with the dip one in Fig. 2(a).

With the transmission spectra for the LCP and the RCP waves, the corresponding CD spectra can be calculated with Eq. (1) and are depicted in Figs. 2(c)(d). Results show that the maximum value reaches $CD = 0.59$ at $f = 0.91 \text{ THz}$ for the dielectric VO_2 state and $CD = -0.51$ at $f = 0.96 \text{ THz}$ for the metallic VO_2 state. Strikingly, at 0.97 THz the circular dichroism of the

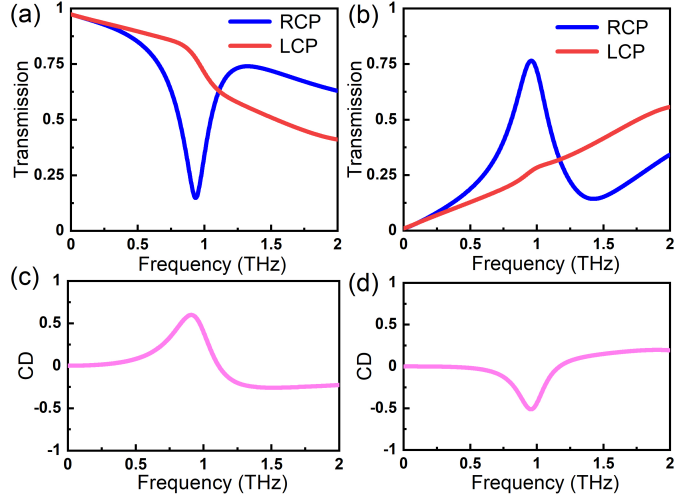


Figure 2: (a)(b) Simulated transmission spectra $|t(f)|$ for LCP and RCP waves and (c)(d) the corresponding circular dichroism when VO₂ is in the (a)(c) dielectric or (b)(d) metallic state.

proposed metasurface switches reversely between 0.5 and -0.5 when VO₂ transits between the dielectric state and the metallic state.

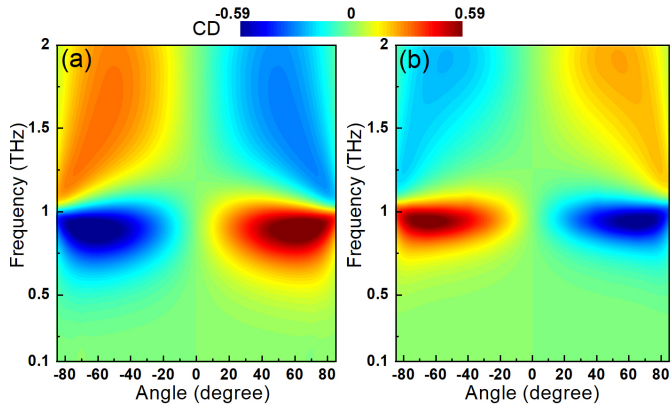


Figure 3: CD spectra for various incident angles between -85° and 85° for (a) VO₂(D) and (b) VO₂(M).

In order to understand the physics underlying the reversible and strong CD effect of the proposed metasurface, we first calculated the dependence of CD spectra on the incident angle and plotted the results in Fig. 3. We find that under normal incidence ($\theta = 0^\circ$), the proposed metasurface exhibits no CD effect regardless of the operation frequency and the VO₂ state (dielectric or metallic). This suggests that the CD effect of the proposed metasurface is not intrinsic. As the incidence angle increases, the CD effect first becomes pronounced and then gradually decreases for frequencies around $f = 0.95$ THz. The CD spectra are anti-symmetric with respect to the $\theta = 0^\circ$ axis. Figs. 3(a)(b) for the dielectric and the metallic VO₂ states are slightly different. These differences arise because metallic VO₂ with $\sigma = 4 \times 10^5$ S/m cannot behave the same as gold, and dielectric VO₂ as well as the substrate also affects the performances. The maximum CD values are ± 0.59 at $f = 0.91$ THz and $\theta = \pm 60^\circ$ for the dielectric VO₂ state, and ± 0.51 at $f = 0.96$ THz and $\theta = \pm 60^\circ$ for the metallic VO₂ state. The strong angular dependence indicates that the CD effect in the proposed metasurface belongs to extrinsic chirality.

To further understand the distinct transmission and strong CD effect for the LCP and the RCP waves with oblique incidence of $\theta = 60^\circ$, in Fig. 4 we plot the current distributions of the proposed metasurface with dielectric VO₂ at $f = 0.94$ THz. Results show that for the RCP wave, strong counterclockwise currents are excited in the U-shaped VO₂ structures, whereas for the LCP

wave, weak clockwise currents are excited. The strong resonance for the RCP wave results in the transmission dip, whereas the weak one for the LCP wave leads to high transmission. These explain the large difference in transmission in Fig. 2(a) and the large CD effect in Fig. 2(c). The transmission difference in Fig. 2(b) and the large but reverse CD effect in Fig. 2(d) can also be explained similarly.

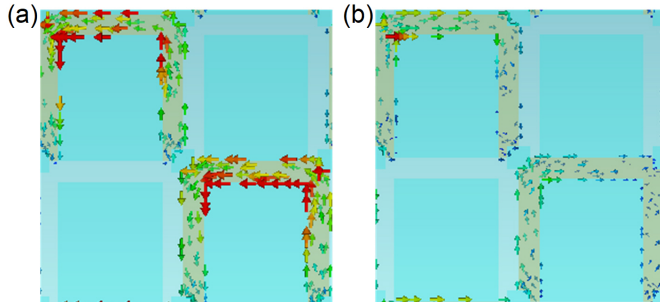


Figure 4: Current distributions in the metasurface unit cell with $\text{VO}_2(\text{D})$ for (a) RCP and (b) LCP waves. The calculations were performed with $\theta = 60^\circ$ and $f = 0.94$ THz.

The reversible CD effect in the proposed Babinet-invertible chiral metasurface can be understood by the electric and magnetic field distributions for the resonant frequencies of the LCP and the RCP waves when VO_2 transits between the dielectric and the metallic state. Figs. 5(a)(b) show that electric and magnetic fields are confined to the U-shaped gold structures when VO_2 is in the dielectric state. However, when VO_2 is in the metallic state, electric and magnetic fields are confined to the U-shaped slots, as shown by Figs.5(c)(d). By comparing Figs. 5(a)(d) [or (b)(c)], we find the electric (or magnetic) field for dielectric VO_2 has similar distributions as the magnetic (or electric) field for metallic VO_2 . These similarities are consistent with complementary structures designed according to the Babinet principle in the literature [30].

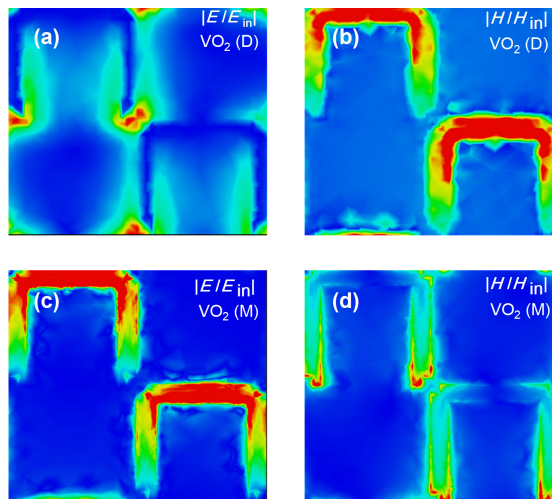


Figure 5: (a)(c) Electric field and (b)(d) magnetic field distributions in the metasurface unit cells under obliquely incident RCP wave. The calculations were performed with $\theta = 60^\circ$, and (a)(b) $f = 0.94$ THz for $\text{VO}_2(\text{D})$ and (c)(d) $f = 0.96$ THz for $\text{VO}_2(\text{M})$.

Until now we have fixed the VO_2 conductivities for the dielectric and the metallic states, in experiments, however, the conductivities of the as-fabricated VO_2 films may vary significantly [31]. Hereafter we investigate the effects of the VO_2 conductivities on the transmission and CD spectra for $\theta = 60^\circ$. Fig. 6(a) shows that as the VO_2 conductivity increases from $\sigma = 40$ S/m to 4×10^6 S/m, the transmission spectra for the RCP first show a dip with decreasing strength and red-shifting frequency, and then exhibit a peak with increasing amplitude and blue-shifting frequency. Interestingly, when $\sigma = 4 \times 10^3$ S/m, the transmission spectrum for the LCP wave almost overlaps with that for the RCP wave. Correspondingly, the peak CD evolves from 0.59 for

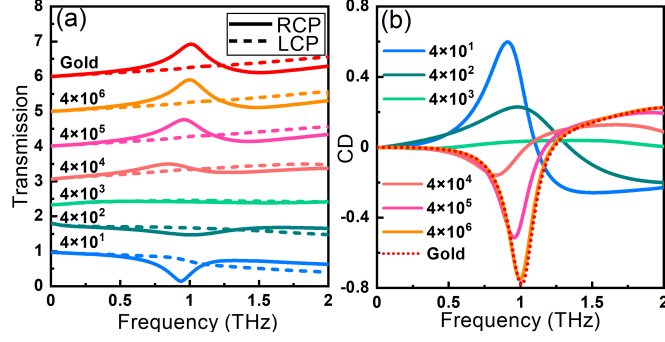


Figure 6: (a) Transmission spectra and (b) CD spectra for various conductivities of VO_2 , which are taken to vary from 40 S/m to $4 \times 10^6 \text{ S/m}$. As a comparison, we also plot the spectra when VO_2 is replaced by gold.

$\sigma = 40 \text{ S/m}$, to near zero $\sigma = 4 \times 10^3 \text{ S/m}$, and to -0.75 for $\sigma = 4 \times 10^6 \text{ S/m}$. Therefore, results suggest that in order to achieve strong and reversible CD tuning beyond ± 0.5 for the proposed metasurface, the conductivity difference between the dielectric and metallic VO_2 should be three or four orders of magnitude. This requires high quality deposited VO_2 films, which were reported by Yun *et al.* [32] and also by the authors quite recently [31].

As a comparison, we also calculated the transmission and the CD spectra when VO_2 is replaced by gold, the conductivity of which is $\sigma = 4.56 \times 10^7 \text{ S/m}$ in the CST build-in library. We find that these spectra overlap well with those when the conductivity of VO_2 is $\sigma = 4 \times 10^6 \text{ S/m}$. In other words, if the conductivity of VO_2 is above $4 \times 10^6 \text{ S/m}$, it can be effectively treated as gold.

In conclusion, we have proposed a Babinet-invertible chiral metasurface to achieve reversible and strong CD effect. Simulation results have shown that, when VO_2 transits between the dielectric state and the metallic state, the transmission spectrum for the RCP wave is flipped, from exhibiting a dip to showing a peak. Correspondingly, the CD switches between 0.5 and -0.5 at 0.97 THz . The angular dependent CD spectra have shown that the CD effect of the proposed metasurface is extrinsic. The near-field distributions have revealed that the equivalent metasurface unit cells for dielectric and metallic VO_2 are complementary structures satisfying the Babinet principle. By investigating the influences of the VO_2 conductivity on the CD tuning performance, we have shown that three or four orders of magnitude large difference between the VO_2 conductivities for the dielectric state and the metallic state is required to achieve the large CD tuning range. We expect the proposed Babinet-invertible chiral metasurface will provide a new strategy for realizing active and tunable optical chirality and will find applications in polarization dependent fields.

Acknowledgments

This work was supported by Shenzhen Fundamental Research and Discipline Layout project (JCYJ20180507182444250) and China Postdoctoral Science Foundation (2020M682984).

References

- [1] Shengyan Yang, Zhe Liu, Sha Hu, Ai Zi Jin, Haifang Yang, Shuang Zhang, Junjie Li, and Changzhi Gu. Spin-selective transmission in chiral folded metasurfaces. *Opt. Lett.*, 6(4):3432–3439, 2019.
- [2] Yoon Young Lee, Ryeong Myeong Kim, Sang Won Im, Mani Balamurugan, and Ki Tae Nam. Plasmonic metamaterials for chiral sensing applications. *Nanoscale*, 12:58–66, 2019.
- [3] Quan Guo, Yuan Zhang, Zhihui Lyu, Dongwen Zhang, Yindong Huang, Chao Meng, Zengxiu Zhao, and Jianmin Yuan. THz time-domain spectroscopic ellipsometry with simultaneous measurements of orthogonal polarizations. *IEEE Trans. Terahertz Sci. Technol.*, 9(4):422–429, 2019.

- [4] Won Jin Choi, Gong Cheng, Zhengyu Huang, Shuai Zhang, Theodore B Norris, and Nicholas A Kotov. Terahertz circular dichroism spectroscopy of biomaterials enabled by kirigami polarization modulators. *Nat. Mater.*, 18(8):820–826, 2019.
- [5] Guan Ke, Ai Bo, Peng Bile, He Danping, Lin Xue, Wang Longhe, Zhong Zhangdui, and Kürner Thomas. Scenario modules, ray-tracing simulations and analysis of millimetre wave and terahertz channels for smart rail mobility. *IET Microw.*, 12(4):501–508, 2017.
- [6] Sang Soon Oh and Ortwin Hess. Chiral metamaterials: enhancement and control of optical activity and circular dichroism. *Nano Converg.*, 2(24):24, 2015.
- [7] Fei Xie, Wei Wu, Mengxin Ren, Wei Cai, and Jingjun Xu. Lattice collective interaction engineered optical activity in metamaterials. *Adv. Opt. Mater.*, 8(2):1901435, 2020.
- [8] Yuanyuan Huang, Zehan Yao, Fangrong Hu, Changji Liu, Leilei Yu, Yanping Jin, and Xinlong Xu. Tunable circular polarization conversion and asymmetric transmission of planar chiral graphene-metamaterial in terahertz region. *Carbon*, 119:305–313, 2017.
- [9] Yang Zhao, MA Belkin, and A Alù. Twisted optical metamaterials for planarized ultrathin broadband circular polarizers. *Nat. Commun.*, 3(1):870, 2012.
- [10] Mark D Turner, Matthias Saba, Qiming Zhang, Benjamin P Cumming, Gerd E Schröder-Turk, and Min Gu. Miniature chiral beamsplitter based on gyroid photonic crystals. *Nat. Photon.*, 7(10):801–805, 2013.
- [11] Mario Hentschel, Martin Schäferling, Xiaoyang Duan, Harald Giessen, and Na Liu. Chiral plasmonics. *Sci. Adv.*, 3(5):e1602735, 2017.
- [12] Frank Neubrech, Mario Hentschel, and Na Liu. Reconfigurable plasmonic chirality: Fundamentals and applications. *Adv. Mater.*, 32(41):1905640, 2020.
- [13] Anton Kuzyk, Robert Schreiber, Hui Zhang, Alexander O Govorov, Tim Liedl, and Na Liu. Reconfigurable 3D plasmonic metamolecules. *Nat. Mater.*, 13(9):862–866, 2014.
- [14] Xiang Lan, Tianji Liu, Zhiming Wang, Alexander O Govorov, Hao Yan, and Yan Liu. DNA-guided plasmonic helix with switchable chirality. *J. Am. Chem. Soc.*, 140(37):11763–11770, 2018.
- [15] Shuang Zhang, Jiangfeng Zhou, Yong Shik Park, Junsuk Rho, Ranjan Singh, Sunghyun Nam, Abul K Azad, Hou Tong Chen, Xiaobo Yin, Antoinette J Taylor, and Xiang Zhang. Photoinduced handedness switching in terahertz chiral metamolecules. *Nat. Commun.*, 3(1):1–7, 2012.
- [16] George Kenanakis, Rongkuo Zhao, N Katsarakis, M Kafesaki, CM Soukoulis, and EN Economou. Optically controllable THz chiral metamaterials. *Opt. Express*, 22(10):12149–12159, 2014.
- [17] Xinghui Yin, Martin Schäferling, Ann Katrin U Michel, Andreas Tittl, Matthias Wuttig, Thomas Taubner, and Harald Giessen. Active chiral plasmonics. *Nano. Lett.*, 15(7):4255–4260, 2015.
- [18] TT Lv, YX Li, HF Ma, Z Zhu, ZP Li, CY Guan, JH Shi, H Zhang, and TJ Cui. Hybrid metamaterial switching for manipulating chirality based on VO₂ phase transition. *Sci. Rep.*, 6:23186, 2016.
- [19] Sheng Xiang Wang, Lei Kang, and Douglas H Werner. Active terahertz chiral metamaterials based on phase transition of vanadium dioxide (VO₂). *Sci. Rep.*, 8(1):189, 2018.
- [20] A Papakostas, A Potts, DM Bagnall, SL Prosvirnin, HJ Coles, and NI Zheludev. Optical manifestations of planar chirality. *Phys. Rev. Lett.*, 90(10):107404, 2003.
- [21] E Plum, VA Fedotov, and NI Zheludev. Extrinsic electromagnetic chirality in metamaterials. *J. Opt. A: Pure Appl. Opt.*, 11(7):074009, 2009.

- [22] SeokJae Yoo and Q Han Park. Metamaterials and chiral sensing: a review of fundamentals and applications. *Nanophotonics*, 8(2):249–261, 2019.
- [23] Heonyeong Jeong, Younghwan Yang, Hanlyun Cho, Trevon Badloe, Inki Kim, Ren Min Ma, and Junsuk Rho. Emerging advanced metasurfaces: Alternatives to conventional bulk optical devices. *Microelectron. Eng.*, 220(15):111146, 2020.
- [24] Yuttana Intaravanne and Xianzhong Chen. Recent advances in optical metasurfaces for polarization detection and engineered polarization profiles. *Nanophotonics*, 9:1003–1014, 2020.
- [25] Zhong Huang, Kan Yao, Guangxu Su, Wei Ma, Lin Li, Yongmin Liu, Peng Zhan, and Zhenlin Wang. Graphene-metal hybrid metamaterials for strong and tunable circular dichroism generation. *Opt. Lett.*, 43(11):2636–2639, 2018.
- [26] Shaoen Zhou, Pengtao Lai, Hua Dong, Guo, Ping Li, Yuxiang Li, Zheng Zhu, Chunying Guan, and Jinhui Shi. Tunable chiroptical response of graphene achiral metamaterials in mid-infrared regime. *Opt. Express*, 27(11):15359–15367, 2019.
- [27] Zewei Shao, Xun Cao, Hongjie Luo, and Ping Jin. Recent progress in the phase-transition mechanism and modulation of vanadium dioxide materials. *NPG Asia Mater.*, 10:581–605, 2018.
- [28] F Falcone, T Lopetegi, MAG Laso, JD Baena, J Bonache, M Beruete, R Marqués, Ferran Martín, and M Sorolla. Babinet principle applied to the design of metasurfaces and metamaterials. *Phy. Rev. Lett.*, 93(19):197401, 2004.
- [29] Yanhan Zhu, Yong Zhao, Mark Holtz, Zhaoyang Fan, and Ayrton A Bernussi. Effect of substrate orientation on terahertz optical transmission through VO₂ thin films and application to functional antireflection coatings. *J. Opt. Soc. Am. B*, 29(9):2373–2378, 2012.
- [30] Andreas Bitzer, Alex Ortner, Hannes Merbold, Thomas Feurer, and Markus Walther. Terahertz near-field microscopy of complementary planar metamaterials: Babinet’s principle. *Opt. Express*, 19(3):2537–2545, 2011.
- [31] Xiaoxiang Dong, Xiaoqing Luo, Yixuan Zhou, Yuanfu Lu, Fangrong Hu, Xinlong Xu, and Guangyuan Li. Switchable broadband and wide-angular terahertz asymmetric transmission based on a hybrid metal-VO₂ metasurface. *Opt. Express*, 28:30675–30685, 2020.
- [32] Sun Jin Yun, Jung Wook Lim, JongSu Noh, ByungGyu Chae, and HyunTak Kim. Vanadium dioxide films deposited on amorphous SiO₂-and Al₂O₃-coated Si substrates by reactive RF-magnetron sputter deposition. *Jpn. J. Appl. Phys.*, 47(4S):3067, 2008.